

The impact of EDGES 21-cm data on dark matter interactions

Kingman Cheung^{a,b,c}, Jui-Lin Kuo^a, Kin-Wang Ng^{d,e}, and Yue-Lin Sming Tsai^d

^a*Department of Physics, National Tsing Hua University, Hsinchu 30013, Taiwan*

^b*Physics Division, National Center for Theoretical Sciences, Hsinchu 30013, Taiwan*

^c*Division of Quantum Phases and Devices, School of Physics,
Konkuk University, Seoul 143-701, Republic of Korea*

^d*Institute of Physics, Academia Sinica, Taipei 11529, Taiwan*

^e*Institute of Astronomy and Astrophysics,
Academia Sinica, Taipei 11529, Taiwan*

Abstract

The recently announced results on 21-cm absorption spectrum by EDGES can place very interesting constraints on the dark matter annihilation cross sections and corresponding channels. We properly take into account all the annihilation from the radiation epoch to the 21-cm observation redshifts in the Boltzmann code for the cosmic microwave background. Our results show that one can use the 21-cm absorption profile to constrain the dark matter interactions for the first time. For DM annihilation into the e^+e^- channel, the EDGES results give the most stringent upper limit on the annihilation cross section at the lower dark matter mass region comparing with other existing limits.

I. INTRODUCTION

Big Bang theory is the most accepted theory for the beginning of the Universe. Our knowledge of science in various disciplines can more or less predict the evolution of the Universe from the earliest time $t \sim 10^{-43}$ s since the Big Bang to the current epoch. One of the key ingredients – inflation – in the theory has been established by observation of the cosmic microwave background (CMB) in 90’s [1].

The CMB, also called the “afterglow” of the Big Bang, was the earliest light coming out from the soup of free electrons, protons, neutrons, and nuclei. Only when the free electrons were caught by protons, neutrons, and nuclei to form neutral atoms, mostly hydrogen and helium, the photons can shine through the matter and form the CMB. It happened about 380,000 years after the Big Bang. Such footprints of the early Universe can tell us a lot of information about the ingredients of the Universe.

Subsequently, the WMAP in the last decade firmly established the idea of inflation and pinned down the valid parameters of the most popular cosmological model, namely, the Λ CDM model [2]. The Planck collaboration [3] continued the mission of measuring more precisely the model parameters in this decade, and also some more parameters that were not able to be measured previously, such as CMB polarization.

After the recombination epoch, the Universe entered into the so-called dark ages, containing mainly neutral hydrogen gas, and everything is very quiet. It is believed that during this period the dark matter (DM) first began to cluster to form halos and thus the gravitational potential for the normal matters to fall in to form structures. The Universe then entered into the “reionization” epoch when the first galaxy or star was being formed. The Gunn-Peterson test on quasar absorption lines has however revealed that the Universe has been reionized at redshift $z \sim 7$ [4]. More precise measurements of the reionization bump in the CMB E -mode polarization power spectrum have inferred an optical depth integrated to the recombination, $\tau \sim 0.08$, and a full reionization at $z \sim 9$ [3]. Nevertheless, how the reionization happened and when exactly it happened are uncertain. It is generally believed that radiation from first stars and/or galaxies ionize the neutral gas beginning at $z \sim 15 - 20$ [5].

A direct measurement of the reionization is made possible owing to the hyperfine splitting of neutral hydrogen atoms, which emit or absorb photons of wavelength at 21-cm in the rest frame dependent on the spin temperature of the hydrogen gas, T_s . This spin temperature

is determined by the background temperatures of the CMB (T_γ) as well as the surrounding thermal gas (T_g). Thus, measurements of redshifted 21-cm lines allow us to perform a tomographic study of the reionization process. There have been a lot of observational efforts to map the primeval hydrogen gas distributions; current experiments include LOFAR, MWA, SKA, and many more [5]. Recently, the experiment EDGES has detected the monopole signal of 21-cm absorption [6], opening a new chapter of the 21-cm cosmology.

EDGES has claimed that the measured amplitude of the 21-cm absorption profile is more than a factor of two greater than the largest predictions [6]. To explain this anomaly, one may have to reduce the spin temperature T_s by introducing new light-DM interactions to cool down the gas [7–12]. An alternative way is to add a strong radio background such that the effective T_γ is higher than the original CMB temperature [13–16]. These two approaches put very interesting requirements on the properties of the DM if the anomaly is indeed due to new DM physics.

In this work, instead of explaining the anomaly, we take the surface value of the EDGES results to constrain DM annihilation in the early Universe. If the DM annihilation into standard model (SM) particles such as quarks, leptons, and photons, it will heat up the gas and increase the gas temperature T_g . Since T_s somewhat traces T_g , the DM annihilation will affect the evolution of T_s and thus also the T_{21} signal probed by EDGES. Until the point where T_s is raised to a value beyond the allowed range of the EDGES results, the DM annihilation rate would be excluded by the data. Therefore, the 21-cm measurements can become a very important tool in current and future experiments to constrain the DM annihilation rates and corresponding channels.

II. METHODOLOGY

EDGES has recently measured an absorption feature for 21-cm emission [6]. At the redshift $z = 17.2$, the temperature T_{21} at 99% confidence level (C.L.) is reported by

$$T_{21}^{\text{EDGES}} = -500_{-500}^{+200} \text{ mK}, \quad (1)$$

where the errors $_{-500}^{+200}$ mK present the systematic uncertainties.

On the other hand, the theoretical prediction is given by

$$T_{21}(z) \simeq 23\text{mK} \left[1 - \frac{T_\gamma(z)}{T_s(z)} \right] \left(\frac{\Omega_b h^2}{0.02} \right) \left(\frac{0.15}{\Omega_m h^2} \right) \sqrt{\frac{1+z}{10}} x_{HI}, \quad (2)$$

where $\Omega_b h^2$ and $\Omega_m h^2$ are the relic densities of baryon and matter, respectively. The number fraction of neutral hydrogen x_{HI} is approximately equal to $1 - x_e$, where x_e is the ionization fraction. The photon temperature $T_\gamma(z)$ can be the same as the CMB temperature, $T_{CMB} = 2.7(1+z)\text{K}$, and the spin temperature $T_s(z)$ controls the atomic excitation between the $s = 0$ and $s = 1$ states of the neutral hydrogen. The value of $T_s(z)$ lies between the gas temperature and the CMB temperature. Therefore, the precise value of $T_s(z)$ would be sensitive to the heated gas from DM annihilation. Here we take the null DM-signal approach ¹ to constrain the DM parameter space.

In the early Universe, DM annihilates or decays into SM particles and ultimately produces some amounts of energetic electrons/positrons (e^-/e^+) and gamma rays (γ). Those of high-energy e^\pm and γ can ionize, heat, and excite the hydrogen atoms. We follow the formalism and methodology developed in Ref. [18], which does not rely on any assumption on the energy fractions f_{eff} as used in most of the literature. The DM contribution to the ionization fraction of hydrogen atom (x_e) via DM annihilation is

$$-\left[\frac{dx_e}{dz}\right]_{\text{DM}} = \sum_{\text{ch}} \int_z \frac{dz'}{H(z')(1+z')} \frac{n_\chi^2(z')}{2n_H(z')} \langle\sigma v\rangle \mathcal{B}(z') \text{BR}_{\text{ch}} \frac{m_\chi}{E_{\text{Ry}}} \frac{d\chi_i(\text{ch}, m_\chi, z', z)}{dz}, \quad (3)$$

and the gas temperature T_g is modified as

$$-\left[\frac{dT_g}{dz}\right]_{\text{DM}} = \sum_{\text{ch}} \int_z \frac{dz'}{H(z')(1+z')} \frac{n_\chi^2(z')}{3n_H(z')} \langle\sigma v\rangle \mathcal{B}(z') \text{BR}_{\text{ch}} m_\chi \frac{d\chi_h(\text{ch}, m_\chi, z', z)}{dz}, \quad (4)$$

where the subscript 'ch' represents the DM annihilation or decay channels with the branching ratio BR_{ch} and i or h refers to ionization or heating. Note that in the above expressions the energy is injected by DM annihilation at redshift z' while absorbed by the neutral hydrogen at redshift z . We define the parameters: the Rydberg energy $E_{\text{Ry}} = 13.6\text{eV}$, the DM mass m_χ , DM annihilation cross section $\langle\sigma v\rangle$, the DM number density n_χ , and the number density of the hydrogen atoms n_H . The fraction of injected energy for a given m_χ and an annihilation channel 'ch' can be obtained by integrating out the energy E ,

$$\frac{d\chi_{i,h}(\text{ch}, m_\chi, z', z)}{dz} = \int dE \frac{E}{m_\chi} \left[2 \frac{dN_e(\text{ch}, m_\chi)}{dE} \frac{d\chi_{i,h}^{(e)}(E, z', z)}{dz} + \frac{dN_\gamma(\text{ch}, m_\chi)}{dE} \frac{d\chi_{i,h}^{(\gamma)}(E, z', z)}{dz} \right], \quad (5)$$

¹ The null DM-signal approach has been widely used in several DM astrophysical limits such as the AMS02 positron constraint [17].

where the injected energy fractions for electron and photon are, respectively,

$$\frac{d\chi_{i,h}^{(e)}(E, z', z)}{dz} \quad \text{and} \quad \frac{d\chi_{i,h}^{(\gamma)}(E, z', z)}{dz}, \quad (6)$$

given by Ref. [18].² The energy spectrum per DM annihilation at the source, $\frac{dN_e(\text{ch}, m_\chi)}{dE}$ for electrons and $\frac{dN_\gamma(\text{ch}, m_\chi)}{dE}$ for photons, are calculated by LikeDM [19] by using the tables from PPPC4 [20]. Similar to Ref. [21], we also introduce a cosmological boost factor \mathcal{B} to account for the effect of DM inhomogeneities and structures [22],

$$\mathcal{B}(z') = 1 + \frac{1.6 \times \text{erfc}[(1+z')/20.5]}{(1+z')^{1.54}} \times 10^5. \quad (7)$$

After all the ingredients are included, we insert Eqs. (3) and (4) into the RECFAST code [23] to obtain the DM-modified matter temperature $T_g(z)$. Assuming that T_s is fully coupled to T_g at $z = 15 - 20$ as indicated by the T_{21} signal probed by EDGES, we obtain the DM-modified spin temperature $T_s(z)$ by adding the difference between the two T_g 's with and without DM annihilation to T_s predicted from the EDGES T_{21} signal.

Assuming that the residual measurement is dominated by the first stars and DM can only contribute sub-dominantly, one can invert Eq. (2) to obtain T_s , in which DM does not contribute much. In Fig. 1, we present the best-fit residual model for T_{21} [6] (lower panel) after the foreground is properly removed. In the upper panel of Fig. 1, we present the resulted T_s by comparing with T_{CMB} . In such an approach, the data-derived T_s can be a first-star model-independent input, which can lead to more conservative upper limits on DM annihilation.

There was not enough likelihood information given in Ref. [6]. However, Ref. [7] claimed that the standard value predicted by the first-star model $T_{21} = -209$ mK is 3.8σ away from the experimental value $T_{21}^{\text{EDGES}} = -500$ mK. By assuming a Gaussian distribution, one can obtain approximately the standard deviation as $\sigma_{\text{EDGES}} = (500 - 209)/3.8$ mK and hence the likelihood can be rewritten as

$$\mathcal{L} \propto \exp\left[-\frac{\chi^2}{2}\right], \quad \text{where} \quad \chi^2 = \frac{(T_{21}^{\text{EDGES}} - T_{21}^{\text{TH.}})^2}{\sigma_{\text{EDGES}}^2}.$$

² We thank Masahiro Kawasaki, Kazunori Nakayama, and Toyokazu Sekiguchi for providing us the tables.

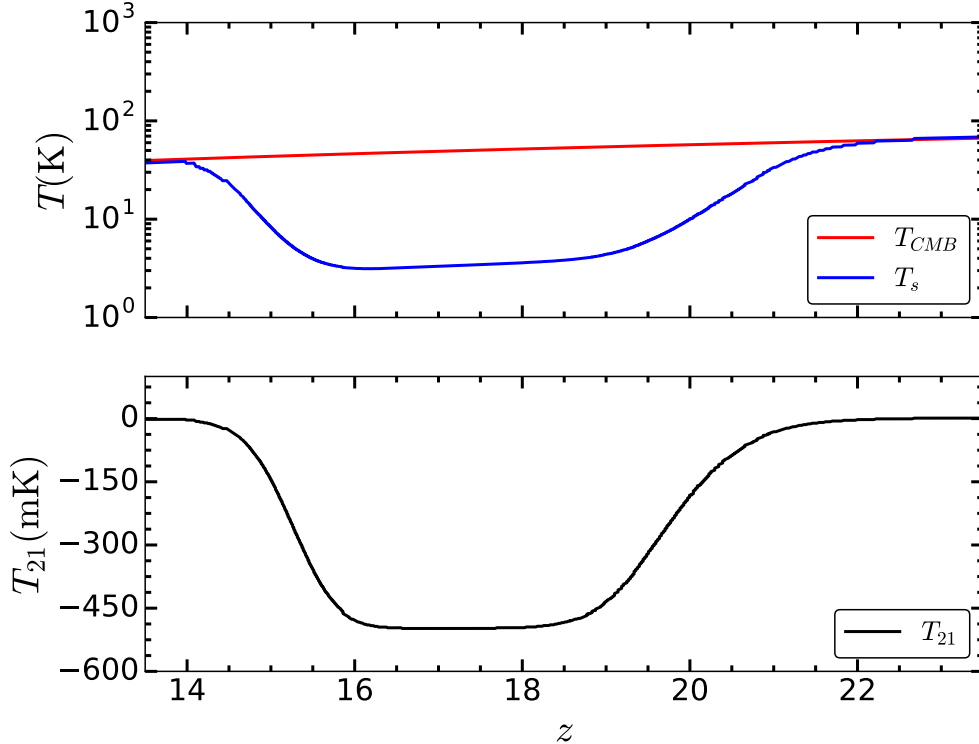


FIG. 1: The best-fit model for T_{21} (lower panel) given in the extended data in Fig. 8 of Ref. [6]. The upper panel presents the T_s which is converted from the best-fit model of T_{21} by assuming a null DM search.

Ω_Λ	H_0	Ω_b	$\Omega_b h^2$	$\Omega_c h^2$	τ	n_s
0.6844	67.27	0.0492	0.02225	0.1198	0.079	0.9645

TABLE I: The cosmology parameters used in this work. Ω_Λ , H_0 , Ω_b , h , Ω_c , τ , and n_s are the energy density parameter of cosmological constant, Hubble constant, energy density parameter of baryon, reduced Hubble constant, energy density parameter of DM, optical depth, and scalar spectral index, respectively.

III. RESULTS

In this section, we first discuss qualitatively the impact of DM annihilation on the gas temperature T_g and the ionization fraction x_e . Then we present the total modification to T_{21} due to DM annihilation. Finally, we present our likelihood analysis in $(m_\chi, \langle\sigma v\rangle)$ parameter space. We adopt the cosmological parameters used in the `CAMB` code [24] as listed in Table I. The cosmological parameters are the central values given in Planck collaboration [3]. Here we

ignore the inherent uncertainties in these parameters because the EDGES T_{21} experimental errors dominate the uncertainties of the current analysis.

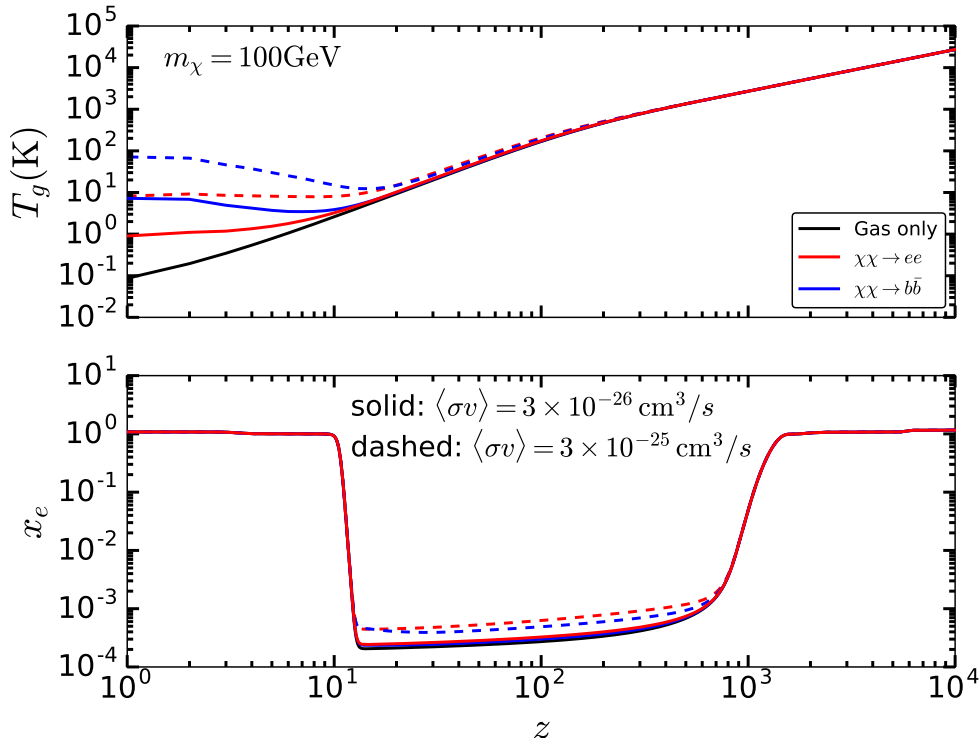


FIG. 2: The evolution of the ionization fraction x_e (lower panel) and the gas temperature T_g (upper panel) for different cases. The black solid line denotes the evolution of T_g without DM annihilation. The red lines represent the modified T_g temperatures with DM annihilation process $\chi\chi \rightarrow e^+e^-$ while the blue lines represent those with DM annihilation process $\chi\chi \rightarrow b\bar{b}$. Different line styles (solid or dashed) stand for different values of $\langle\sigma v\rangle$ ($3 \times 10^{-26} \text{ cm}^3 \text{ s}^{-1}$ or $3 \times 10^{-25} \text{ cm}^3 \text{ s}^{-1}$).

In Fig. 2, we show the evolution of the ionization fraction x_e (lower) and the gas temperature T_g (upper) for DM annihilation to e^+e^- (red) and $b\bar{b}$ (blue), in which the case without DM injection is also shown for comparison in black solid lines. In the lower panel, we can see approximately linear dependence on the cross section at z larger than a few hundreds, which is an important feature of the DM CMB constraints near the recombination epoch [25–27]. However, during the reionization epoch ($z \sim 20$) the linearity disappears and the behavior becomes strongly dependent on the DM property and the injected energy propagation. In the redshift region below $z = 10$, where T_{21} is completely governed by the first stars, we rely

on the default model in CAMB for the x_e computation.

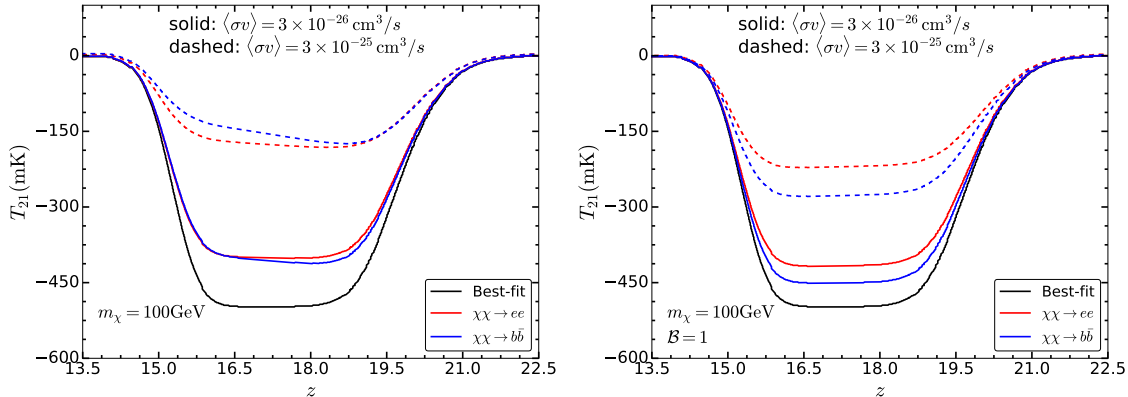


FIG. 3: The comparison of the effects from different DM annihilation channels and cross sections on the T_{21} signal. We compare the cases with the boost factor given by Eq. (7) (left panel) and without the boost factor (right panel). The black solid line is the T_{21} signal from EDGES. The red lines represent the modified T_{21} temperatures with DM annihilation process $\chi\chi \rightarrow e^+e^-$ while the blue lines represent those with DM annihilation process $\chi\chi \rightarrow b\bar{b}$. Different line styles (solid and dashed) stand for different values of $\langle\sigma v\rangle$ ($3 \times 10^{-26} \text{ cm}^3\text{s}^{-1}$ and $3 \times 10^{-25} \text{ cm}^3\text{s}^{-1}$).

In the upper panel of Fig. 2, one can see that the DM contribution becomes dominant in the evolution of T_g at $z \lesssim 30$. More energetic electron-positron pairs and photons can propagate a further distance before they are absorbed, namely, energy absorption into the gas in lower-redshift region more likely comes from lower-energy electron-positron pairs and photons being created in the gas neighborhood. Hence, there are two factors that explain the growth of the $b\bar{b}$ contribution over the e^+e^- channel in heating the gas. First, the DM annihilation to $b\bar{b}$ can yield more lower-energy electron-positron pairs and photons than the e^+e^- channel. Second, the low-energy electron-positron pairs and photons created at low redshifts will be shortly absorbed and successively affecting the present Universe. In contrast, the high-energy electron-positron pairs can travel through the gas without being absorbed. This can be also seen from that $T_g(\chi\chi \rightarrow e^+e^-)$ departs slightly more from T_g (without DM) at larger redshifts than $T_g(\chi\chi \rightarrow b\bar{b})$. Later, the boost factor can largely enhance the annihilation contribution at low redshifts, leading to higher $T_g(\chi\chi \rightarrow b\bar{b})$ temperatures at low redshifts.

In Fig. 3, we compare the experimental best-fit model of T_{21} with those T_{21} of four different DM annihilation scenarios. We also consider two cases, one with the boost factor

(left panel) and the other one without (right panel). As explained previously, the effect of low-energy electron-positron pairs or photons can be easily seen in the EDGES because of their short propagation length. In addition, the boost factor, Eq. (7), can largely enhance such an effect at low redshifts. Hence, we expect that T_{21} at small z should be more altered by $\chi\chi \rightarrow b\bar{b}$ than $\chi\chi \rightarrow e^+e^-$. When comparing the results from $\chi\chi \rightarrow b\bar{b}$ and $\chi\chi \rightarrow e^+e^-$, we found that the boost factor is not so effective for DM annihilation to the e^+e^- final state.

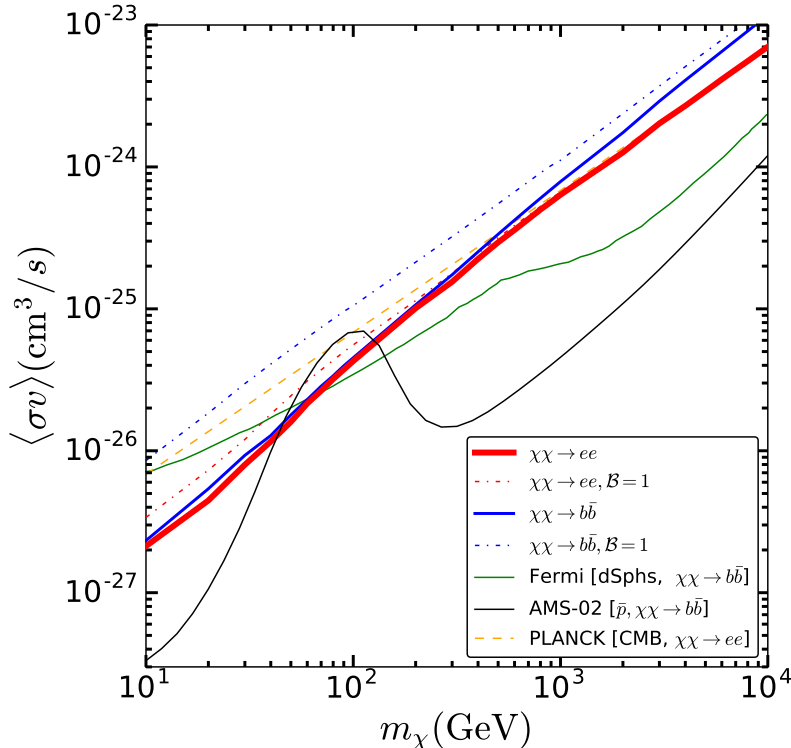


FIG. 4: The 95% upper limits on the DM annihilation cross sections versus the DM mass derived by fitting EDGES data. The DM annihilation final state is assumed to be e^+e^- (red lines) or $b\bar{b}$ (blue lines). The dash-dotted lines are without boost factors. The exclusion limits from PLANCK CMB (orange dashed line), Fermi dSphs (green solid line), and AMS02 antiproton data (black solid line) are also shown for comparison.

Finally, we present the 95% exclusion limit in the $(m_\chi, \langle\sigma v\rangle)$ plane based on EDGES data in Fig. 4. For each DM mass bin, we normalize the maximum likelihood to one and depict a solid line in 95% C.L. corresponding to $-2\Delta \ln \mathcal{L} = 2.71$ for a one-sided Gaussian likelihood distribution. The red thick line presents the the limit based on the assumption that DM annihilates to the e^+e^- final state while the blue thin line is for the $b\bar{b}$ final state. As

comparison, we also take the 95% C.L. upper limit on $\chi\chi \rightarrow b\bar{b}$ from the Fermi observation on dwarf galaxies [28] (green thin line) and the AMS02 antiproton fitting [29, 30] (black thin line). However, for the PLANCK CMB measurement [3] (orange dashed line), we only show the limit for $\chi\chi \rightarrow e^+e^-$ since the limit for $b\bar{b}$ channel is too weak when compared with the others.

With the boost factor, one can see that the e^+e^- channel is only slightly more stringent than the $b\bar{b}$ channel in the lower-mass region but it becomes stronger at the larger mass region. However, for the case without the boost factor (thin dash-dotted line), the e^+e^- channel is overall a factor of 2 – 3 more stringent than the $b\bar{b}$ channel. Interestingly, the boost factor does not affect the e^+e^- channel as significantly as the $b\bar{b}$ channel. This is totally due to the fact that the more energetic electron-positron pairs or photons will be absorbed in a longer distance as aforementioned. At large DM mass region $m_\chi \gtrsim 500$ GeV, one can see no difference in the e^+e^- channel between the cases with and without the boost factor.

Comparing with the PLANCK CMB constraints (for the effects in $z \sim 600 - 1100$), both the e^+e^- and $b\bar{b}$ channels for our EDGES limits are stronger than those for PLANCK CMB. When comparing with the Fermi dSph data, the EDGES limit for the $b\bar{b}$ channel is stronger than the Fermi constraint in the low-mass region ($m_\chi \leq 80$ GeV) while weaker at higher masses. However, if the boost factor is removed, the EDGES limit is no longer stronger than the Fermi limit. On the other hand, the AMS-02 antiproton constraint is in general stronger than the EDGES limit for the $b\bar{b}$ channel even when the boost factor is included, except for a small mass window ($m_\chi = 30 - 200$ GeV). Overall, for a thermal DM relic whose annihilation is through a s -wave (velocity independent) process with a standard value of $\langle\sigma v\rangle \sim 3 \times 10^{-26} \text{ cm}^3 \text{ s}^{-1}$, the EDGES limits can exclude both e^+e^- and $b\bar{b}$ channels in the mass region $m_\chi \leq 100$ GeV at 95% C.L.

Note that the statistics between our constraints and those in Ref. [21] is clearly different. In Ref. [21], the constraints are obtained by demanding that the standard value of the 21-cm absorption ($T_{21} = -200$ mK) is not washed out by the DM annihilation by half the amount ($\Delta T_{21} \leq 100$ mK). On the other hand, our analysis are based on the best-fit model of the EDGES T_{21} signal to derive the constraints on the DM annihilation. Although our limits are slightly weaker than those in Ref. [21], our results do not rely on any *ad hoc* energy fractions f_{eff} . We have also shown the effects of the boost factor $\mathcal{B}(z)$ on different DM annihilation

channels, which indicate that the approximation via f_{eff} may be invalid in reckoning the contribution of DM annihilation. More importantly, we do not assume immediate absorption of electrons, positrons, and photons during the propagation from z' to z .

IV. CONCLUSIONS

Regarding the absorption signal of 21-cm line probed by the EDGES experiment, we have adopted the null DM-signal assumption to derive the modified evolution of T_{21} by considering DM annihilation into e^+e^- and $b\bar{b}$ final states. In this approach, one can simply bypass the unclear model uncertainties of the formation of first stars. We have further assumed that the process of DM annihilation is velocity independent (s -wave) and considered the boost factor as for approximating the enhancement of DM annihilation in the cosmic structures. Being different from other studies that mainly rely on the assumption of DM annihilation efficiency in terms of energy fractions f_{eff} , we have adopted the methodology developed in Ref. [18], which directly computes the propagation of the injected energy and does not assume any f_{eff} in the calculation. We have utilized the tabulated propagation kernels in Ref. [18] to calculate the rate of change of the ionization fraction and the gas temperature for both e^+e^- and $b\bar{b}$ channels. Note that it is precise enough to obtain CMB constraints by using f_{eff} , since the CMB constraints mainly come from high-redshift annihilation where the linearity still exists. However, for lower redshifts relevant to the 21-cm absorption signal, the linearity breaks down due to the formation of structures, and thus the assumption of using a simple f_{eff} may not be adequate. We have shown the effects of the boost factor on the e^+e^- and $b\bar{b}$ channels and found that the enhancement of the boost factor is larger for the $b\bar{b}$ channel due to the fact that the $b\bar{b}$ final state produces more low-energy electron-positron pairs and photons after a sequence of cascading decays. With the modified T_{21} evolution, we have derived the constraints on the e^+e^- and $b\bar{b}$ channels, which are comparable to the constraints from the Fermi dSphs data and the AMS-02 antiproton data. As expected, our EDGES limit for the e^+e^- channel is slightly more stringent than that for the $b\bar{b}$ channel. Nevertheless, with the enhancement of the boost factor, the EDGES limit for the $b\bar{b}$ channel is almost tantamount to that for e^+e^- .

In the future, if the EDGES global 21-cm signal is confirmed and more experimental data on 21-cm sky fluctuations are obtained, the 21-cm observation will become a standard

tool to constrain DM interactions as indicated by our results. At last, a better study on the evolution of the spin temperature will benefit deriving more realistic systematic uncertainties that may further improve our constraints.

Acknowledgments

Y.S.T. would like to thank Kazunori Nakayama for kindly explaining their tables and many email exchanges. This work was supported in part by the Ministry of Science and Technology, Taiwan, ROC under Grants No. MOST-104-2112-M-001-039-MY3 (K.W.N.) and MOST-105-2112-M-007-028-MY3 (K.C.).

-
- [1] N. W. Boggess et al., *Astrophys. J.* **397**, 420 (1992).
 - [2] G. Hinshaw et al. (WMAP), *Astrophys. J. Suppl.* **208**, 19 (2013), 1212.5226.
 - [3] P. A. R. Ade et al. (Planck), *Astron. Astrophys.* **594**, A13 (2016), 1502.01589.
 - [4] J. E. Gunn and B. A. Peterson, *Astrophys. J.* **142**, 1633 (1965).
 - [5] J. R. Pritchard and A. Loeb, *Rept. Prog. Phys.* **75**, 086901 (2012), 1109.6012.
 - [6] J. D. Bowman, A. E. E. Rogers, R. A. Monsalve, T. J. Mozdzen, and N. Mahesh, *Nature* **555**, 67 EP (2018), URL <http://dx.doi.org/10.1038/nature25792>.
 - [7] R. Barkana, *Nature* **555**, 71 EP (2018), URL <http://dx.doi.org/10.1038/nature25791>.
 - [8] J. B. Muñoz and A. Loeb (2018), 1802.10094.
 - [9] R. Barkana, N. J. Outmezguine, D. Redigolo, and T. Volansky (2018), 1803.03091.
 - [10] A. Berlin, D. Hooper, G. Krnjaic, and S. D. McDermott (2018), 1803.02804.
 - [11] A. Fialkov, R. Barkana, and A. Cohen (2018), 1802.10577.
 - [12] S. Fraser et al. (2018), 1803.03245.
 - [13] C. Feng and G. Holder (2018), 1802.07432.
 - [14] A. Ewall-Wice, T. C. Chang, J. Lazio, O. Dore, M. Seiffert, and R. A. Monsalve (2018), 1803.01815.
 - [15] J. Mirocha and S. R. Furlanetto (2018), 1803.03272.
 - [16] M. Pospelov, J. Pradler, J. T. Ruderman, and A. Urbano (2018), 1803.07048.

- [17] L. Bergstrom, T. Bringmann, I. Cholis, D. Hooper, and C. Weniger, *Phys. Rev. Lett.* **111**, 171101 (2013), 1306.3983.
- [18] M. Kawasaki, K. Nakayama, and T. Sekiguchi, *Phys. Lett.* **B756**, 212 (2016), 1512.08015.
- [19] X. Huang, Y.-L. S. Tsai, and Q. Yuan, *Comput. Phys. Commun.* **213**, 252 (2017), 1603.07119.
- [20] M. Cirelli, G. Corcella, A. Hektor, G. Hutsi, M. Kadastik, P. Panci, M. Raidal, F. Sala, and A. Strumia, *JCAP* **1103**, 051 (2011), [Erratum: *JCAP*1210,E01(2012)], 1012.4515.
- [21] G. D'Amico, P. Panci, and A. Strumia (2018), 1803.03629.
- [22] C. Evoli, A. Mesinger, and A. Ferrara, *JCAP* **1411**, 024 (2014), 1408.1109.
- [23] S. Seager, D. D. Sasselov, and D. Scott, *Astrophys. J.* **523**, L1 (1999), astro-ph/9909275.
- [24] A. Lewis, A. Challinor, and A. Lasenby, *Astrophys. J.* **538**, 473 (2000), astro-ph/9911177.
- [25] X.-L. Chen and M. Kamionkowski, *Phys. Rev.* **D70**, 043502 (2004), astro-ph/0310473.
- [26] T. R. Slatyer, N. Padmanabhan, and D. P. Finkbeiner, *Phys. Rev.* **D80**, 043526 (2009), 0906.1197.
- [27] C. Evoli, M. Valdes, A. Ferrara, and N. Yoshida, *Mon. Not. Roy. Astron. Soc.* **422**, 420 (2012).
- [28] A. Albert et al. (DES, Fermi-LAT), *Astrophys. J.* **834**, 110 (2017), 1611.03184.
- [29] M.-Y. Cui, Q. Yuan, Y.-L. S. Tsai, and Y.-Z. Fan, *Phys. Rev. Lett.* **118**, 191101 (2017), 1610.03840.
- [30] M.-Y. Cui, X. Pan, Q. Yuan, Y.-Z. Fan, and H.-S. Zong (2018), 1803.02163.